

# Toughness Measurements on Steel Fibre-reinforced High Strength Concrete

M. Taylor, F. D. Lydon & B. I. G. Barr

Division of Civil Engineering, Cardiff School of Engineering, University of Wales Cardiff, Cardiff, UK

(Received 22 March 1996; accepted 5 August 1997)

## Abstract

*The paper reports on strength and toughness measurements on a range of normal and high strength concrete mixes, with and without steel fibre reinforcement. Cube strength, modulus of rupture, cylinder splitting and torsional-tension test results are reported together with toughness measurements determined via two fracture-type test specimens (standard RILEM three-point notched beams in flexure and eccentrically loaded notched cubes). In the toughness tests, crack mouth opening displacement (CMOD) was measured and used in a closed loop testing mode to achieve complete load/displacement curves. Good correlation was observed in the strength tests and the two toughness tests showed similar load–CMOD curves and toughness indices. However, traditional toughness indices are unsatisfactory with load–CMOD tests, and further work is necessary to define acceptable toughness measurements, which may also have to account for size effects. The effect of steel fibre reinforcement on high strength (up to 120 N/mm<sup>2</sup>) and normal strength concrete is similar. © 1997 Elsevier Science Ltd. All rights reserved.*

**Keywords:** High strength concrete, toughness, fibre-reinforced concrete, fracture tests, strength tests, toughness indices.

## INTRODUCTION

The 1990s has been a period of increasing research interest in the area of high strength concrete (HSC) where the cube strength is in the range 70–120 N/mm<sup>2</sup>. This interest is due

partly to the increasing use of HSC in construction and partly to the inherent durability benefits of such materials. Furthermore, there are many examples of economic advantages in using concrete with strengths well in excess of the normal design strength values. These advantages must be balanced not only against costs but also against the increased relative brittleness of HSC. Hence, there is a significant amount of research being carried out at the present time to investigate the effect of adding fibres to improve the ductility of HSC.

The toughness of fibre-reinforced concrete (FRC) materials can be considered as their energy absorption capacity, which is usually characterised by some portion of the area under the load-displacement curve obtained during a flexure test. Most toughness measurements have been performed on un-notched beams in flexure using a four-point loading arrangement. A review of the essential features of such tests has been given recently by Gopalaratnam and Gettu.<sup>1</sup> Their review describes the range of toughness measurements (energy-based dimensionless indices, energy absorption capacity, strength-based dimensionless indices, residual strength indices, equivalent flexural strength and deflection-based dimensionless indices) in European, North American and Japanese standards.

The most widely reported toughness measurements are the energy-based dimensionless toughness indices. Essentially, the practical application of such indices began with the introduction of the ACI Toughness Index,<sup>2</sup> based on the work of Henegar.<sup>3</sup> ACI Committee 544 defined the toughness index as the ratio of the amount of energy required to deflect a fibre

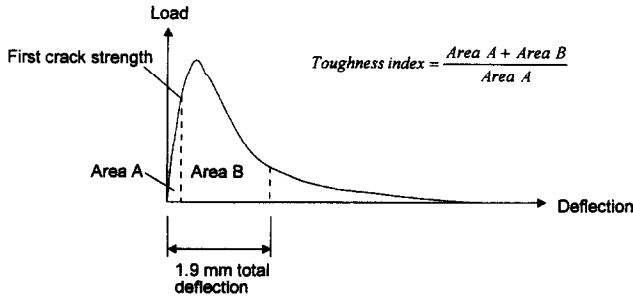
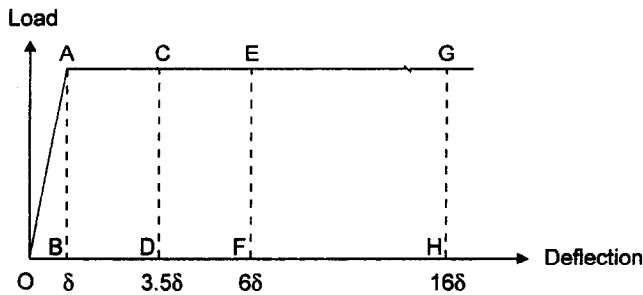


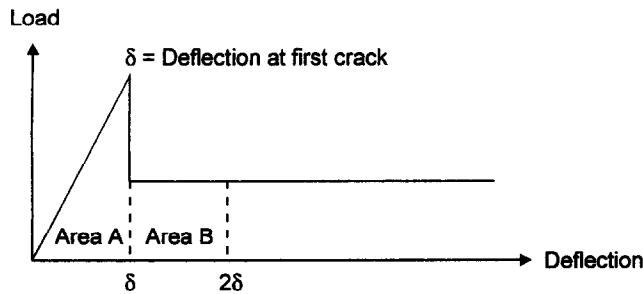
Fig. 1. Definition of ACI toughness index.<sup>2</sup>

concrete beam by a prescribed amount to the energy required to bring the fibre beam to the point of first crack (Fig. 1). A similar approach was adopted with the development of the ASTM C 1018 standard,<sup>4</sup> based on the work of Johnston.<sup>5</sup> In this standard, toughness indices are evaluated for a number of prescribed deflections based on multiples of the first-crack deflection (Fig. 2). The toughness index proposed by Barr and Hasso<sup>6</sup> is similar to that of the Johnston/ACI 544 proposal as it is based on the ratio of two areas under the load–deflection curve up to twice the deflection at first-crack (Fig. 3). Significantly, this toughness index was



$$\text{Toughness index } (I_5) = \frac{ACDB}{OAB}, \quad (I_{10}) = \frac{AEFB}{OAB}$$

Fig. 2. Definitions of ASTM C 1018 toughness indices.<sup>4</sup>



$$\text{Toughness index} = \frac{\text{Area B}}{3 \times \text{Area A}} \times 100\%$$

Fig. 3. Definition of Toughness Index by Barr and Hasso.<sup>6</sup>

proposed for and has been applied to both notched and un-notched specimens subjected to various loading arrangements.

Current standards/guidelines for the evaluation of the toughness characteristics of FRC materials have a number of limitations,<sup>1</sup> which include:

- the wide range of parameters that have been used to interpret test results,
- the greater variation in the recorded deflections in four-point bend tests compared with three-point bend tests,
- the difficulty of determining accurately the location of first crack,
- the exaggerated deflections recorded via the testing machine relative to the actual net central deflection of the test specimens and
- the influence of size effects on the test results.

It has been proposed recently<sup>7</sup> that many of the above limitations can be overcome by evaluating toughness via notched beams, subjected to three-point loading, as proposed in the  $G_F$  test recommendation.<sup>8</sup> Furthermore, it has been proposed that the deformation of the test specimens should be measured directly from the specimen rather than through the testing machine. This can best be achieved by recording the crack mouth opening displacement (CMOD) rather than the net central deflection via a ‘yoke’ arrangement.<sup>7</sup> Such an approach has been adopted in the work reported here.

## STRENGTH AND TOUGHNESS TESTING DETAILS

The 28-day compressive strength was determined by means of 100-mm cubes and three test methods were used to evaluate the corresponding tensile strength. Two traditional tensile strength tests (modulus of rupture,  $f_b$ , and the split cylinder,  $f_s$ ) were used together with a new indirect tensile strength test, based on a beam specimen subjected to torsional loading,<sup>9</sup> as shown in Fig. 4. The torsional loading creates shear stresses on a plane perpendicular to the beam's longitudinal axis. These shear stresses together with the associated complementary shear stresses result in tensile stresses acting at 45° to the longitudinal axis of the beam. It has been shown<sup>9</sup> that the

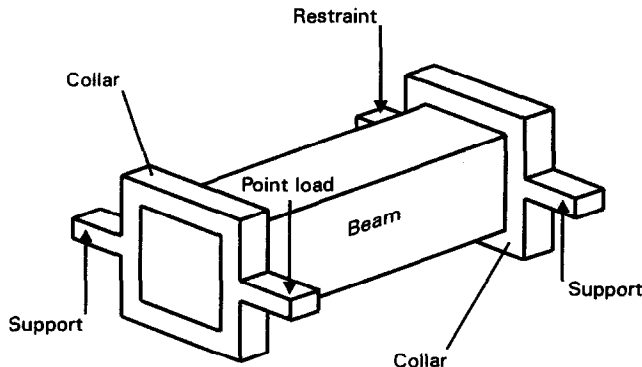


Fig. 4. Schematic view of torsional loading arrangement.

maximum shear stress,  $\tau_{max}$ , for the beams is given by:

$$\tau_{max} = M_t / 0.208d^3,$$

where  $M_t$  is the applied torque, and  $d$  is the beam width or depth. The maximum shear stresses occur at the mid-point of the width or depth of the sides in a square section. At any given section, the shearing stresses vary along the edge of the boundary, from a maximum at the mid-point to zero at the corners. Thus, the shearing stresses determined according to the above formula will give an upper limit for the indirect tensile strength of the concrete.

Toughness measurements have also been carried out as part of this study. Probably the most widely used toughness standard is the ASTM C 1018 standard,<sup>4</sup> illustrated in Fig. 2. This standard has been used to evaluate the test results reported here and requires the location of the first-crack,  $\delta_f$  which is significantly more difficult than that suggested by the schematic figure given in Fig. 2. Having located  $\delta_f$ , a number of toughness indices ( $I_5$ ,  $I_{10}$  and  $I_{20}$ ) corresponding to increasing portions of the post-first-crack curves can be determined. The portion of the load-deflection curve to be considered is determined in terms of multiples of the first-crack deflection;  $I_5$  corresponds to 3.5  $\delta_f$ ,  $I_{10}$  corresponds to 6  $\delta_f$ , and  $I_{20}$  corresponds to 11  $\delta_f$ . (The subscripts are used since an elastic-plastic response for the load-deflection curve would yield toughness indices with these values.)

Some of the limitations of the ASTM C 1018 standard have been reported by Banthia *et al.*<sup>10</sup> who introduced a frame (or 'yoke') around their flexural beam specimens that allowed direct measurement of the net central deflection of the beam. The use of a yoke eliminated extraneous deflections and resulted in load-

deflection curves that were significantly different from those observed by using the traditional cross-head displacement of so-called stiff testing machines. According to Banthia *et al.*, it is only by using a yoke-type arrangement that the real deflection of the flexure beam can be determined. The problems associated with the various current definitions of toughness indices, as described by Banthia *et al.*, can be overcome by combining the notion of toughness indices with tests on notched specimens used extensively by the concrete fracture community.<sup>8</sup>

Currently, three test methods<sup>8,11,12</sup> for evaluating the fracture characteristics of concrete are under consideration. In one of these test methods,<sup>8</sup> the fracture energy of concrete,  $G_F$ , is determined via stable tests carried out on centrally notched beam specimens wherein the actual deflection of the beam is recorded rather than the apparent deflection recorded by the testing machine. In the second of the proposed fracture tests, the Two-parameter Method<sup>11</sup>, fracture is assumed to be governed by the two parameters of critical stress intensity factor and the critical crack tip opening displacement (CTOD), which is also measured directly off the test specimen. This notion of measuring displacement directly off the test specimen rather than via the testing machine, which is well developed and accepted practice in fracture tests, has been a major influence on the experimental work reported here.

The experimental approach reported above has been made possible due to the rapid changes that have taken place with testing machines in recent years. Until recently, toughness tests were traditionally carried out in stiff testing machines that allowed deflection control only. More recently, many research laboratories have been using closed-loop testing systems in order to achieve stable fracture tests in concrete specimens. In such machines, the deflection recorded by the opening of the crack (or notch) mouth is used to control the test itself. Apart from achieving stable fracture tests, the closed-loop testing arrangement allows the crack mouth opening displacement (CMOD) to be used directly to monitor the test specimen response.

Some experimental work has already been reported, based on the notions described above. Gopalaratnan *et al.*<sup>13</sup> proposed the use of notched beams, tested under servo-controlled

conditions, to characterise toughness of FRC materials. More recently, Bryars *et al.*<sup>14</sup> tested centrally loaded notched beams of steel fibre reinforced high strength concrete in which the toughness index was defined as the ratio between the areas under the load-CMOD curve until a prescribed multiple of the first-crack and until the first-crack itself. This work has been developed further in a recent paper by Barr *et al.*<sup>7</sup> and is the basis of the work reported here for high-strength, fibre-reinforced concrete.

## EXPERIMENTAL PROGRAMME

### Mix proportions

The experimental work reported here forms part of a study being carried out by the authors on the strength and fracture characteristics of ordinary and high strength concrete. The full study is designed to provide basic data on HSC (with and without fibre reinforcement) manufactured using both gravel and crushed limestone coarse aggregate. Two types of fibres have been used in the study: the results for polypropylene fibre have been reported earlier<sup>9</sup>, and this paper deals specifically with the steel FRC mixes. Optimum fibre content (i.e. enhancement of toughness without introducing significant problems with the workability of the mixes) has been investigated for a range of concrete strengths. The test results presented here have been limited to the crushed limestone mixes, but similar results have been observed with the gravel mixes.

The first phase of the experimental programme required the design of standard

concrete mixes with nominal 28-day cube strengths of 40, 60, 80, 100 and 120 N/mm<sup>2</sup>. This aspect of the work has been reported elsewhere<sup>15</sup> and will not be repeated here. Table 1 gives details of the mix proportions for both the crushed limestone and gravel mixes. The nominal 80, 100 and 120 N/mm<sup>2</sup> mixes contained 10% silica fume (supplied in a 50:50 slurry) by weight of cement. These three mixes also contained Conplast SP430 as a superplasticiser. Throughout this first phase of the programme, careful attention was given to the requirements of workability and the proportion of fine material to allow the inclusion of fibres into the mixes during the next stage of the study.

### Strength and toughness tests

As stated earlier, both strength and toughness tests (based on fracture tests) have been carried out in the study. The compressive strength was determined by means of 100-mm cubes, and the tensile strength was determined by means of three types of indirect tensile tests:

- modulus of rupture,  $f_b$ , via 100 × 100 × 500 mm beams in flexure,
- cylinder splitting strength,  $f_s$ , via 100-mm diameter, 200-mm-long cylinders, and
- torsional-tension strength,  $f_t$ , via 100 × 100 × 500 mm beams subjected to torsion.

The toughness evaluation was carried out via two types of fracture tests. The first toughness test was identical to the  $G_F$  test<sup>8</sup> and is illustrated in Fig. 5. Both ends of the 100 × 100 × 500 mm test beams illustrated in Fig. 5 were pinned with one support free to

Table 1. Mix proportions

Aggregate type	Nominal grade	Mix proportions					
		Cement (kg/m <sup>3</sup> )	Fine aggregate (kg/m <sup>3</sup> )	Coarse aggregate (kg/m <sup>3</sup> )	Water (kg/m <sup>3</sup> )	Silica fume (kg/m <sup>3</sup> )	Superplasticizer (ml/kg of cement)
Limestone	40	400	800	1000	224	—	—
	60	400	724	1124	200	—	—
	80	340	721	1190	170	37	13.5
	100	400	708	1188	140	44	23.0
	120	510	653	1086	122	56	35.9
Gravel	40	400	800	1000	224	—	—
	60	400	724	1124	200	—	—
	80	370	714	1188	159	41	21.5
	100	455	696	1151	132	50	26.5
	120	510	653	1086	122	56	35.9

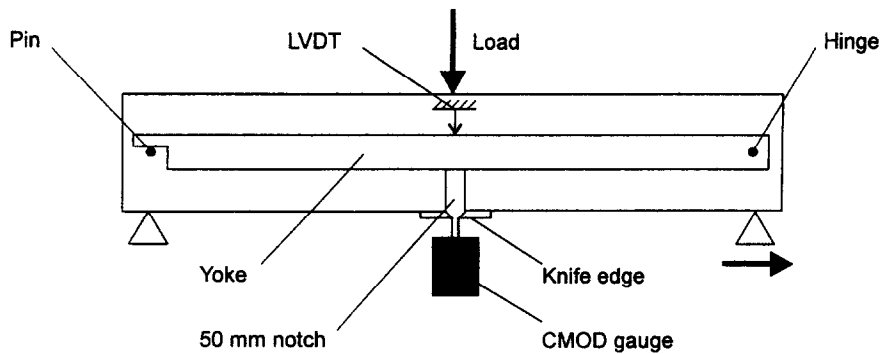


Fig. 5. Loading arrangement for notched beam specimens.

move horizontally. The actual mid-span deflection, measured relative to the beam itself, was recorded by means of a yoke arrangement similar to that used by Bantia *et al.*<sup>10</sup>. Knife edges were attached on either side of the notch on to which a CMOD gauge (which kept the rate of crack mouth opening displacement constant during the test) was fixed. The beams were loaded centrally, and the load–CMOD together with the load–central deflection curves were produced autographically.

The second test used to evaluate the toughness is based on earlier work by Barr *et al.*<sup>16</sup> in which two notches are introduced into cube specimens and fracture is achieved via the eccentric loading arrangement, illustrated in Fig. 6. In this study, the cubes were 150 mm, and the two notches were 50 mm deep leaving a ligament of 50 mm. Knife edges were attached on either side of the notch remote from the loading edge and a CMOD gauge fitted to monitor and measure the CMOD during test. The notched cubes were loaded eccentrically, as shown, and the load–CMOD curves were recorded autographically.

### Preparation of specimens

All mixes were prepared in a 250-kg horizontal pan mixer. For each mix, six plain concrete con-

trol cubes were taken from the mix prior to the addition of the fibres. The fibre content reported here is based on the remaining concrete, after the removal of the material required for the six control cubes. These cubes were tested at 7 days and 28 days to confirm the repeatability of the basic mixes. The steel fibre used in the study was Bekaert Dramix ZL30/.50. Both slump and VeBe time were measured for all mixes prior to casting of the specimens. For each grade of concrete, the initial fibre content was 2% by weight. Thereafter, the fibre content was varied to determine the optimum value based on observations of the mixing process and the results from the workability tests. The optimum fibre content is considered to be the maximum fibre content consistent with an acceptable degree of workability, i.e. the concrete is sufficiently workable to be properly compacted without undue expenditure of energy, say roughly comparable to a VeBe time no greater than about 8–10 s.

The test specimens were compacted on a vibrating table, demoulded on the following day and cured under water, at 20°C, for 27 days. The specimens were notched by a 'Clipper' masonry saw after 27 days and tested at 28 days. The knife edge supports were glued into position immediately after the notches had been introduced into the test specimens.

The experimental programme described above allowed a number of features to be investigated, as follows:

- (1) Effect of steel fibre reinforcement on a range of concrete strengths.
- (2) The use of load–CMOD curves to determine toughness indices (rather than the traditional load–displacement curves).
- (3) A comparison of toughness indices determined from notched beam and notched cube specimens.

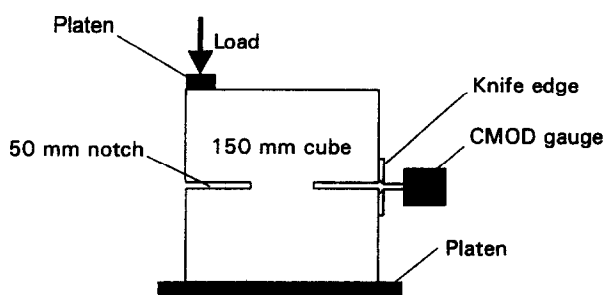


Fig. 6. Loading arrangements for notched cube specimens.

**Table 2.** Workability results

Nominal grade	Fibre content (percentage by volume)	Slump (mm)	Vebe (s)
40	0	140	1
	0.52	100	1
	0.78	90	2
	1.04	65	2
60	0	25	4
	0.26	0	6
	0.39	20	7
	0.52	0	9
80	0	120	1
	0.26	55	3
	0.52	45	3
	0.78	0	8
100	0	65	4
	0.26	45	5
	0.39	35	6
	0.52	10	10
120	0	95	3
	0.26	65	4
	0.39	55	5
	0.52	55	7

**Table 3.** Compressive and tensile strength results

Nominal grade	Fibre content (percentage by volume)	$f_{c28}$ (N/mm <sup>2</sup> )	$f_{b28}$ (N/mm <sup>2</sup> )	$f_{t28}$ (N/mm <sup>2</sup> )	$f_{s28}$ (N/mm <sup>2</sup> )
40	0	43.8	6.6	6.1	3.4
	0.52	42.0	6.9	6.7	4.1
	0.78	44.3	9.1	6.8	5.2
	1.04	47.0	10.9	7.4	5.8
60	0	67.1	8.2	8.7	5.2
	0.26	67.7	7.8	8.6	5.2
	0.39	69.6	8.0	8.2	5.7
	0.52	71.0	9.5	8.8	7.3
80	0	85.3	9.0	9.4	4.5
	0.26	84.7	9.9	9.5	6.8
	0.52	86.0	10.2	9.7	7.0
	0.78	88.6	11.5	10.7	9.7
100	0	104.2	10.8	12.0	6.9
	0.26	104.4	11.1	11.8	7.8
	0.39	104.3	11.8	11.5	8.7
	0.52	107.7	10.9	11.4	8.7
120	0	110.0	13.2	13.2	6.4
	0.26	109.3	13.5	13.1	8.1
	0.39	113.3	13.6	13.9	8.7
	0.52	122.2	12.6	12.4	10.4

## RESULTS AND DISCUSSION

Both slump and VeBe times were measured for all the mixes, and the workability results are presented in Table 2. It is observed that the maximum fibre content, for any given nominal grade of concrete, corresponds to a significant increase in VeBe time. Increasing the fibre volume beyond those reported in Table 2 would result in a poor workability for the FRC mixes. The other test results may be considered in two parts: strength test results and toughness test results.

### Strength results

The results in Table 3 indicate that there is a small increase in compressive strength with increase in fibre content. The increase is generally of the order of a few per cent, with the greatest increase being observed in the case of the Grade 120 concrete. However, great care is required in the interpretation of these results since silica fume and varying amounts of superplasticizer were used with the higher strength mixes. (The results may well be specific to the materials used, in particular to the amounts of SF and SP and their chemistry when combined with the Portland cement.)

The last three columns in Table 3 present the tensile strength results as determined by the

three indirect methods used to evaluate the tensile strength. ( $f_{b28}$  is the tensile strength at 28 days from the modulus of rupture test,  $f_{t28}$  the corresponding result from the torsion-tension test and  $f_{s28}$  the corresponding result from the splitting test.) The tensile strengths evaluated by means of the torsional-loading arrangement,  $f_{t28}$ , are most encouraging and are similar to the tensile strengths evaluated by means of the modulus of rupture testing arrangement. Analysis of the data yields  $f_b = 0.96f_t + 0.39$  (correlation coefficient,  $r = 0.98$  and the number of sets in the analysis,  $n = 18$ ); thus,  $f_b \approx f_t$ . The torsion-tension testing arrangement can be readily reproduced in most testing laboratories and provides a simple method of evaluating tensile strength. This notion can be readily extended to include the testing of cores from real concrete structures. The only difficulty with cores is the need to provide adequate grip between the loading collars and the test specimen. Torsional loading of beams and cylinders, to determine the indirect tensile strength, is currently being pursued in the same laboratory.

Whereas the  $f_{b28}$  and  $f_{t28}$  test results are similar in Table 3, there is a significant difference in the values shown by the cylinder-splitting test results,  $f_{s28}$ . This could be due to the very different stress distributions developed in each test geometry; failure is initiated in the surface of

the modulus of rupture and torsion tests, whereas it is initiated within the body of the test specimen in the case of cylinder-splitting test. Further work is required in this area to establish the reliability of the trends and to produce a sound database for interpretation.

Examination of the cube and flexural tensile results indicates a good correlation, given by  $f_b = 0.51f_c^{0.67}$ , with a correlation coefficient,  $r$ , of 0.93 and number of sets in analysis,  $n = 18$ . Similarly, the relationship between cube and  $f_t$  results shows a good correlation given by

$f_t = 0.30f_c^{0.80}$  with  $r = 0.88$  and  $n = 20$ . For  $f_s$ , the correlation is  $f_t = 0.38f_c^{0.67}$ , with  $r = 0.89$  and  $n = 15$ ; this excludes the plain concrete results, as with polypropylene fibres,<sup>9</sup> for which a separate correlation appears to be applicable.

### Toughness results

Typical load-CMOD curves are shown in Figs 7 and 8 for the notched beam test specimens and in Figs 9 and 10 for the notched cube test specimens. Both test specimens have an uncracked

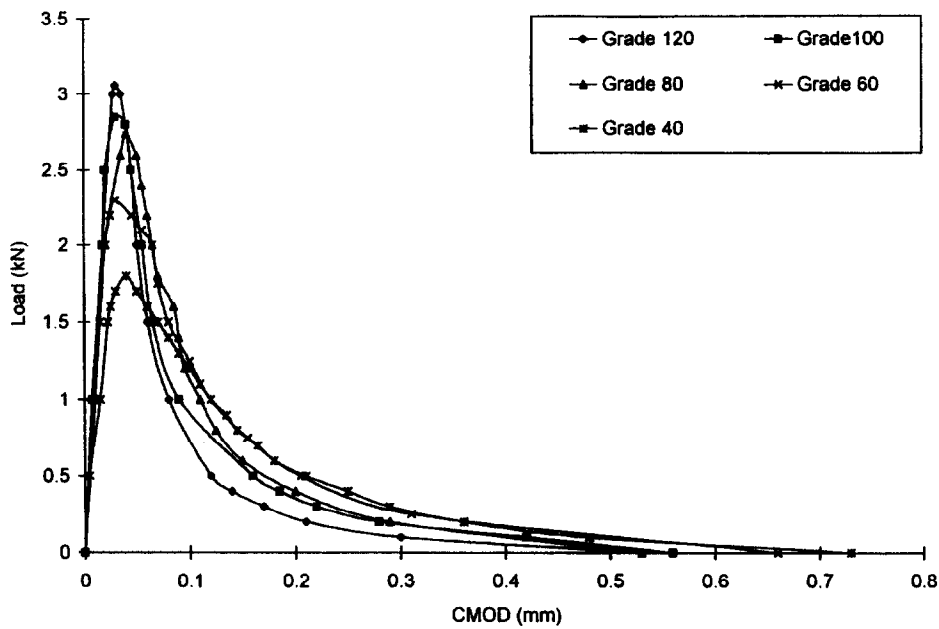


Fig. 7. Typical load-CMOD curves for plain concrete mixes (notched beams).

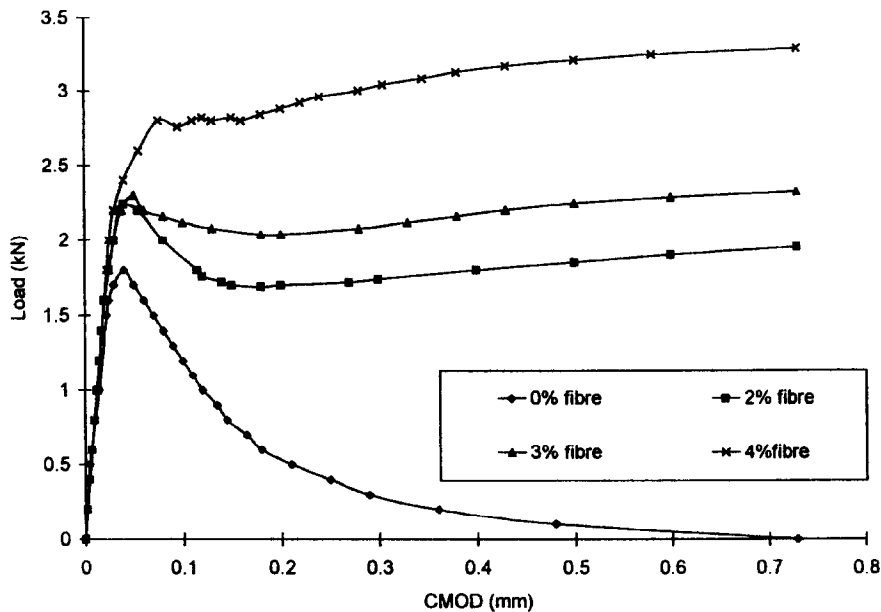


Fig. 8. Typical load-CMOD curves for FRC composite notched beams (nominal 28-day cube strength = 40 N/mm<sup>2</sup>).

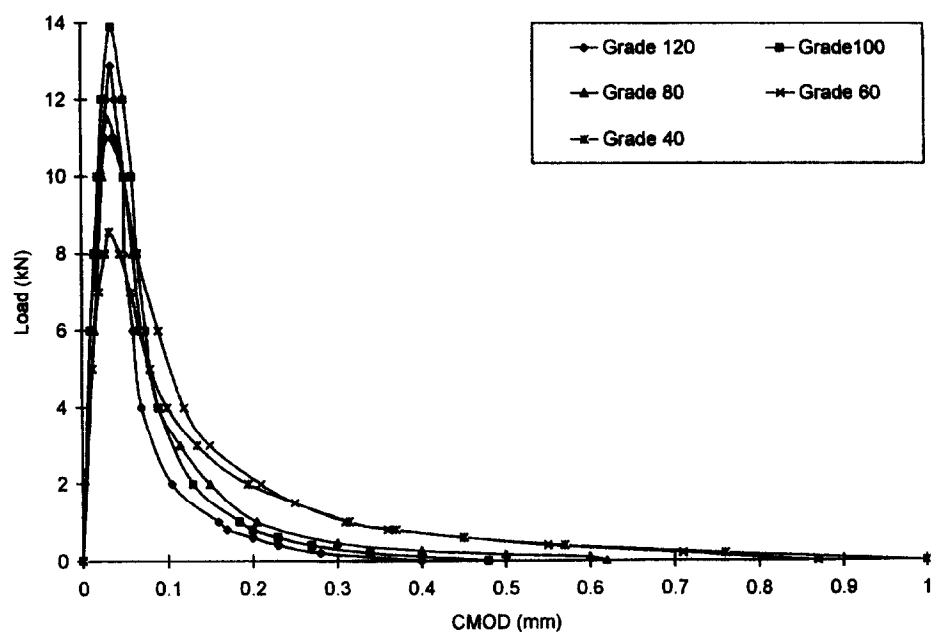


Fig. 9. Typical load-CMOD curves for plain concrete mixes (notched cubes).

ligament length of 50 mm, and the CMOD clip gauge is located 50 mm away from the root of the notch in both cases. Thus, although the testing arrangements are very different, the CMOD measurements are recorded in similar circumstances, and it is only the method of applying the bending moment across the ligament that differs in the two test geometries. Significantly, it is observed that the shape of the load-CMOD curves for the plain concrete mixes is similar for the two geometries and, furthermore, the value of the crack opening

displacement at zero load in the post peak region is also similar for the two geometries. Figures 8 and 10 show the similar effect of the fibre content on the load-CMOD curves for the two test geometries. These two figures suggest that similar load-CMOD curves are obtained when deformation measurements are taken directly off the test specimen geometry, in similar circumstances. It is probable that such direct measurements are more closely related to actual material behaviour than measurements recorded via the testing machine itself.

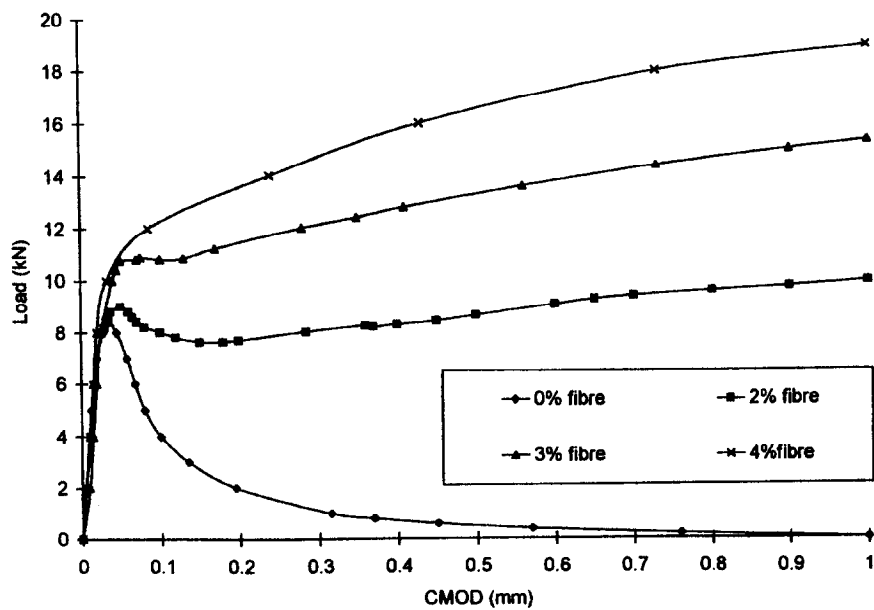


Fig. 10. Typical load-CMOD curves for FRC composite notched cubes (nominal 28 day cube strength = 40 N/mm<sup>2</sup>).



The load-CMOD curves, illustrated in Figs 8 and 10, have been analysed by means of the toughness indices defined in ASTM C 1018. Both the  $I_5$  and  $I_{10}$  indices have been calculated for the two geometries, and the results are presented in Table 4. The  $I_5$  and, in particular, the  $I_{10}$  values calculated using load-CMOD and load-displacement are very similar for all concretes as shown by the results for the beam tests in Table 4. This is as expected given the similar shape of the load-displacement and load-CMOD curves and the method of calculating the toughness indices. As the toughness indices are based upon multiples of the first-crack deflection, the reliable determination of this measure is very important. However, it was difficult to accurately find the point of first-cracking, and as a result, the deflection at peak-load was taken as  $\delta_f$ . As there are several advantages in using the load-CMOD response as a basis for toughness measurement,<sup>13</sup> not least the reduction in errors of measuring CMOD as opposed to deflection, the load-CMOD-derived toughness values are considered the most accurate here, and these alone are therefore discussed further.

For both geometries, the first crack occurs when the CMOD is of the order of 0.04–0.05 mm. Thus, the  $I_5$  and  $I_{10}$  toughness

indices take into account only the area under the curve out to CMOD displacements of approximately 0.175 mm and 0.3 mm, respectively. Although the  $I_5$  and  $I_{10}$  indices are similar for the two geometries, it is clear that neither index extends far enough to capture the enhanced toughness of the steel fibre reinforcement. Unfortunately, this conclusion also applies, even for the  $I_{20}$  toughness index. This aspect of the study shows that a new definition of toughness indices is required to reflect the enhanced toughness properties of FRC composites tested by means of modified fracture tests.

The work reported here supports some earlier conclusions reached by Jamet *et al.*<sup>17</sup>, who tested notched beams under CMOD control to obtain stable load-CMOD curves (for both plain concrete and FRC composites) from which a number of toughness measurements were assessed. Jamet *et al.* claim that their proposed toughness measurements give a better indication of the fundamental behaviour of the concrete, avoid the problems associated with the approach based on the deflection of un-notched beams, and are amenable to the incorporation of serviceability considerations such as crack widths. The main difficulty with the work reported by Jamet *et al.* is the apparent size effect in their test results. The

**Table 4.**  $I_5$  and  $I_{10}$  toughness index results

Nominal grade	Fibre content (percentage by volume)	Notched beam				Notched cube	
		Load/CMOD		Load/ displacement		Load/CMOD	
		$I_5$	$I_{10}$	$I_5$	$I_{10}$	$I_5$	$I_{10}$
40	0	2.6	3.7	2.2	2.9	2.5	3.6
	0.52	3.2	5.9	2.9	5.4	3.4	6.5
	0.78	3.7	7.6	3.4	7.1	3.4	6.9
	1.04	3.9	8.3	4.2	8.8	4.1	8.8
60	0	2.5	3.3	2.0	2.5	2.8	3.8
	0.26	3.3	6.0	3.2	5.8	2.7	5.1
	0.39	3.2	6.0	3.4	6.3	4.1	7.8
	0.52	3.4	6.7	3.7	7.4	3.4	6.8
80	0	2.2	2.8	1.7	2.1	1.8	2.3
	0.26	3.0	5.4	2.7	4.9	3.0	5.3
	0.52	3.4	7.0	3.8	7.7	3.3	6.0
	0.78	4.4	9.5	4.2	9.3	3.9	8.0
100	0	2.5	3.3	1.8	2.3	2.3	2.8
	0.26	3.1	5.2	2.5	4.2	2.4	4.4
	0.39	3.6	6.5	3.6	6.9	3.1	5.8
	0.52	3.3	6.6	2.9	6.0	3.2	5.9
120	0	1.7	2.0	1.4	1.6	1.4	1.6
	0.26	2.7	4.6	2.4	4.2	2.4	3.9
	0.39	2.9	5.4	2.9	5.6	2.9	5.6
	0.52	2.8	5.4	2.9	6.0	2.5	5.0

implications of possible size effects in such toughness measurements require further detailed investigation. The notched cube test specimen provides an obvious choice of test geometry to investigate size effects, due to its compact nature.

The toughness index results given in Table 4 suggest that various testing arrangements can be used to establish the load-CMOD curves for FRC composites. The advantage of using the notched cube geometry rather than the notched beam geometry to study size effects has already been advanced above. Further study is required to determine what difference, if any, is obtained when notched cylinders and/or cores are tested under similar loading arrangements. A comparison of the  $I_5$  and  $I_{10}$  toughness indices for the notched beam and notched cube test specimens is illustrated in Fig. 11. A direct comparison would give a slope of 1.0 for the regression line and a correlation approaching unity. With the exception of the test results for the nominal Grade 60 mixes, a good correlation is observed in Fig. 11 between the test results from the two geometries. Too few results are available to allow the significance to be checked of the correlations for each concrete grade. However, if all the results are pooled, as they are for strengths, it is found that  $I_{5,\text{cube}} = 0.99I_{5,\text{beam}} - 0.2$  (correlation = 0.86,  $n = 20$ ), i.e.  $I_{5,\text{cube}} \approx I_{5,\text{beam}}$ , and  $I_{10,\text{cube}} = 0.94I_{10,\text{beam}} + 0.07$  (correlation = 0.93,  $n = 20$ ). These correlations are significant at better than the 0.1% level. These results suggest that toughness indices determined from CMOD measurements on notched cubes are valid indicators of toughness giving comparable values to those determined in traditional notched beam flexure tests.

## CONCLUSIONS

The effect of adding steel fibres to high strength concrete mixes is similar to that observed in the case of normal strength concrete. The compressive strength is marginally increased with increasing fibre content, with the greatest increase being observed in the case of the Grade 120 concrete. The increase in tensile strength with increasing fibre content is also marginal but more variable, depending upon the test method used to determine the tensile strength. Whereas the increase in tensile

strength evaluated via the split cylinder was significant, the same increase in tensile strength was not observed in the case of the other two test geometries where failure was initiated at the surface of the specimen rather than in the bulk of the specimen. This is probably due to a wall effect whereby the fibre density is less at the surface than in the centre of the test specimens, and further work is required before drawing firm conclusions.

Three methods of evaluating tensile strength were used in the study. An alternative indirect tensile test is described which yields test results that are similar to those given by the modulus of rupture testing arrangement. The similarity of the tensile strengths determined by the modulus of rupture and the torsional loading testing arrangement is probably due to the similarity of crack initiation that occurs at the surface in both cases. The new testing arrangement (which can also be adopted for testing cylinders and cores) requires further investigation and is currently being used in the same laboratory to test specimens under a range of conditions varying from fully saturated to oven dry.

Toughness measurements have been evaluated by means of two fracture-type tests wherein the load-CMOD rather than the load-deflection curves have been used to determine the toughness. Similar toughness results were observed from the two geometries, as in the case of polypropylene FRC mixes reported earlier.<sup>9</sup> Although the  $I_5$  and  $I_{10}$  toughness indices were similar for the two geometries, the results show that neither index extends sufficiently far to capture the enhanced toughness due to fibre reinforcement. Nevertheless, fracture tests using notched test specimens with CMOD deformations measured directly off the test specimens provide a better method of quantifying material behaviour than traditional test methods wherein deformations are recorded via the testing machine. Further research is required to determine what minimum portion of the load-CMOD curves is required to provide sufficient data to monitor toughness.

The results show the potential advantage of the notched cube geometry to study size effects. Earlier work by Jamet *et al.*<sup>17</sup> and Bryars *et al.*<sup>14</sup> has shown a size effect in toughness measurements. The implications of possible size effects in toughness measurements require further detailed investigation using the notched cube

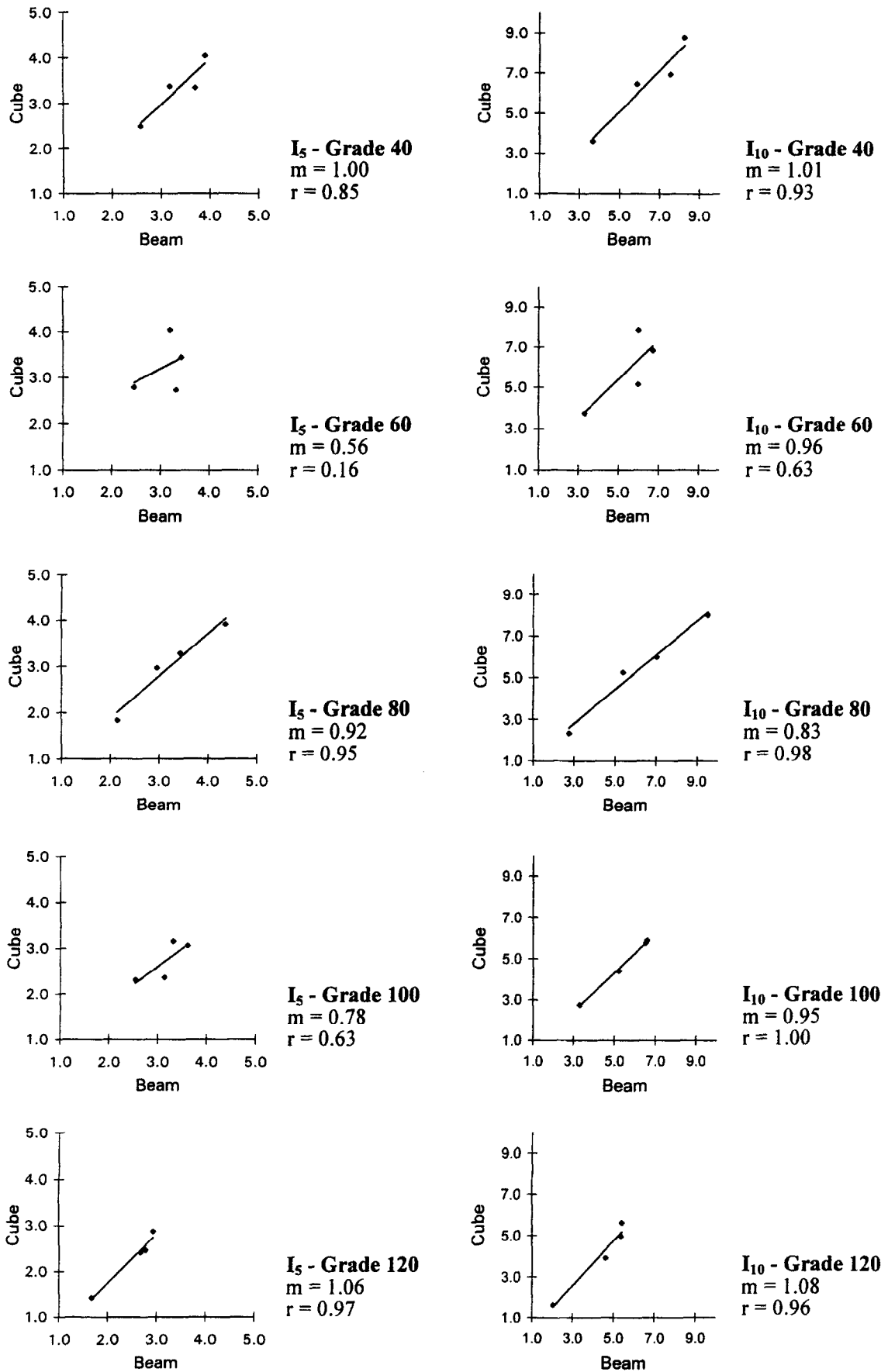


Fig. 11. Comparison of  $I_5$  and  $I_{10}$  toughness indices for notched beams and cubes.

test specimen (rather than the more traditional notched beam in bending) due to its compact nature.

## ACKNOWLEDGEMENTS

The work reported in this paper forms part of an EPSRC Grant (Ref. No. GR/J79379) entitled 'Fracture characteristics of ordinary and high performance concretes by means of relaxation tests'. The authors wish to express their sincere thanks to EPSRC for its support of this work.

## REFERENCES

1. Gopalaratnam, V. S. & Gettu, R., On the characterisation of flexural toughness in FRC. *Cement Concrete Composites*, **17** (1995) 239–254.
2. ACI Committee 544 Measurement of properties of fiber reinforced concrete. *ACI Mater. J.*, **85** (1988) 583–593.
3. Heneger, C. H., Toughness Index of Fibre Concrete. In *Testing and Test Methods of Fibre Cement Composites (RILEM Symposium 1978)*, Construction Press, Lancaster, UK, pp. 79–86.
4. ASTM, Standard Test Method for Flexural Toughness and First-Crack Strength of Fiber-Reinforced Concrete (using Beam with Third-Point Loading), *ASTM C 1018-92*, *ASTM Annual Book of Standards*, Vol. 04.22, ASTM Philadelphia, USA, 1992, pp. 510–516.
5. Johnston, C. D., Definitions and measurement of flexural toughness parameters for fiber reinforced concrete. *Cement, Concrete Aggregate*, **4** (1982) 53–60.
6. Barr, B. & Hasso, E. B. D., A study of Toughness Indices. *Mag. Concrete Res.*, **37** (1985) 162–173.
7. Barr, B., Gettu, T., Al-Oraimi, S. K. A. & Bryars, L. S., Toughness measurement — the need to think again. *Cement Concrete Composites*, **18** (1996) 281–297.
8. RILEM Draft Recommendation, 50FMC Determination of fracture energy of mortars and concrete by means of three-point bend tests on notched beams. *Mater. Struct.*, **18** (1985) 285–290.
9. Barr, B., Taylor, M. & Lydon, F. D., Fracture toughness of high strength fibre reinforced cement composites, *Real World Concrete, Proc. R. N. Swamy Symposium*, ed. Singh, G., Part of Proc. 5th CAN-MET/ACI Int. Conf., Milwaukee, 1995, pp. 145–163.
10. Banthia, N., Trottier, J-F., Wood, D. & Beaupre, D., Steel Fibre reinforced dry-mixture shotcrete. Effect of Fibre geometry on fibre rebound and mechanical properties. *Fibre Reinforced Cement and Concrete, Proc. 4th RILEM Int. Symp.*, ed. Swamy, R. N. E & FN Spon, London, 1992, pp. 277–295.
11. RILEM Draft Recommendation Determinations of fracture parameters ( $K_{Ic}$  and  $CTOD_c$ ) of plain concrete using three-point bend tests. *Mater. Struct.*, **23** (1990) 457–460.
12. RILEM Draft Recommendation Size effect method for determining fracture energy and process zone size of concrete. *Mater. Struct.*, **23** (1990) 461–465.
13. Gopalaratnam, V. S., Shah, S. P., Batson, G. B., Criswell, M. E., Ramakrishnan, V. & Wecharatana, M., Fracture toughness of fiber reinforced concrete. *ACI Mater. J.*, **88** (1991) 339–353.
14. Bryars, L., Gettu, R., Barr, B. & Arino, A., *Fracture of Fiber-Reinforced High-Strength Concrete — A Study Based on Size Effect, Fracture and Damage in Quasi-brittle Structures*, ed. Bazant, Z. P., Bittnar, Z., Jirásek, M. & Mazars, J. E & FN Spon, London, 1994, pp. 319–326.
15. Taylor, M. R., Lydon, F. D. & Barr, B., Mix proportions for high strength concrete. *Construct. Building Mater.*, **10** (1996) 445–450.
16. Barr, B., Evans, W. T. & Dowers, R. C., Fracture toughness of polypropylene fibre concrete. *Int. J. Cement Composites Lightweight Concrete*, **3** (1981) 115–122.
17. Jamet, D., Gettu, R., Gopalaratnam, V. S. & Aguado, A., Toughness of fibre-reinforced high-strength concrete from notched beam tests. To be published in *Testing of Fiber Reinforced Concrete*, ACI Special Publication.